Thin films

DOI: 10.1002/smll.200700680

Polymer Nanocomposite Thin Film Mirror for the Infrared Region**

Thad Druffel, Natalia Mandzy, Mahendra Sunkara, and Eric Grulke*

Thin film metal oxide coatings have been used commercially as electromagnetic filters from the UV to infrared regions for over half a century. Deposition onto a substrate has typically been accomplished using vapor deposition techniques[1–3] and more recently sol–gel methods.[4–7] These coatings provide very good optical and mechanical performance when applied to substrates with similar thermal and mechanical properties. When conventional metal oxide coatings are applied to flexible, relatively soft substrates such as polymers, mismatches in mechanical properties can reduce interfacial adhesion or accelerate mechanical failures.[8,9] The authors recently showed that a thin film polymer nanocomposite can be applied to a polymer substrate and maintain adhesion even under high strains.[10] This paper describes the first time demonstration of an IR mirror using a relatively inexpensive method to apply complicated thin film dielectric stacks to a polymer substrate that can function effectively in high strain systems.

Ultrathin layers of polymer nanocomposites can be used to develop electromagnetic filters, with improved mechanical performance, on compliant substrates such as polymers. Self-assembled polymer nanocomposite thin film layers composed of UV-cured acrylates and metal oxide nanoparticles were developed as antireflective coatings for ophthalmic lenses.[11,12] The primary failure mode in this application is associated with intrinsic stresses introduced during processing and thermal cycling of the plastic. Nanocomposite coatings outperform ceramic coatings on plastic substrates because the primary failures are ductile, limiting secondary cracks propagating from abrasions and thereby reducing haze.[10] Ceramic thin films in similar studies exhibited brittle fracture, which led to secondary cracks and higher haze measurements.[8,9] The use of nanoparticles at high packing densities, up to sixty percent by volume, in a polymer allows for effective refractive index engineering of discrete layers extending from the visible to infrared spectrum.

[*] T. Druffel, Dr. M. Sunkara
Chemical Engineering Department
J.B. Speed School of Engineering University of Louisville
Louisville, KY 40292 (USA)
Fax: (+1) 502-852-6355
E-mail: t0druf01@louisville.edu
N. Mandzy, Dr. E. Grulke
Chemical & Materials Engineering Department, 359 R. G. Anderson Building University of Kentucky Lexington, KY 40506 (USA)

[**] This work was supported by the United States Air Force Research Laboratory under contract number FA8650-05-C-5053 (L. Farrier and S. Szaruga). We also thank Optical Dynamics for their support in this research.

Anti-reflective coatings for the visible range are relatively simple designs of several dielectric layers and are used in many consumer products. These same materials can also be used to create mirrors in the IR region, but the layer counts increases to tens of layers resulting in more complexity in the process. For processes involving dielectric materials, these increased interfaces increase the vulnerability of the coatings to cracking when it is applied to a flexible substrate. A simple thin film filter design utilizes a stack of ¼ wave thickness layers of alternating high and low refractive index materials for which the reflection off a surface is given by Equation 1.

$$R = \left(\frac{(n_0 - Y)}{(n_0 + Y)}\right)^2 \quad (1)$$

where R is reflection, n_0 is index of refraction of air, and Y is admittance of the surface.[13] The admittance of a reflective stack of i alternating ¼ wave high and low refractive index layers is expressed in Equation 2.

$$Y = \frac{n_{high}^{(i+1)}}{n_{sub} n_{low}^{(i-1)}} \quad (2)$$

This simple relationship allows the determination of the filter response at a specified wavelength (λ) having layer thicknesses equal to 0.25 λ/d (d is the optical thickness, which is the product of the refractive index and thickness of the film). The nanocomposite thin films will require more layers than those produced by vacuum deposition since the ratio of refractive indices is less because of the organic binder used in this system.

Reproducible optical response of multilayer filters is only accomplished through precise control of the refractive index and thickness of each layer. In general, preferred layer characteristics include uniform thickness over surface contours, low surface roughness relative to its thickness for sharp differences in refractive index across the layer interfaces, and the highest possible difference in refractive index between adjacent layers maximizing the admittance of the surface. The nanocomposite thin films consist of essentially spherical metal oxide nanoparticles with narrow size distributions dispersed in a continuous matrix of UV-cured acrylate polymer. High transparency and low scattering for each layer require that the nanoparticles are not agglomerated and are significantly smaller in diameter than the waves to be altered. The functional materials and processes described here have allowed our group to achieve the necessary volume densities of nanoparticles without agglomerations.

The packing of the nanoparticles was pushed toward to the theoretical limit of 73% for hexagonal close packing of spheres in order to generate the largest possible refractive index difference between layers. For our set of processing conditions and materials, volume packing of 60% yielded highly reproducible mechanical performance (Figure 1), which is confirmed elsewhere.[14] At this ratio we would expect the refractive index of the layers to follow the rules for nanoparticle–polymer mixtures.

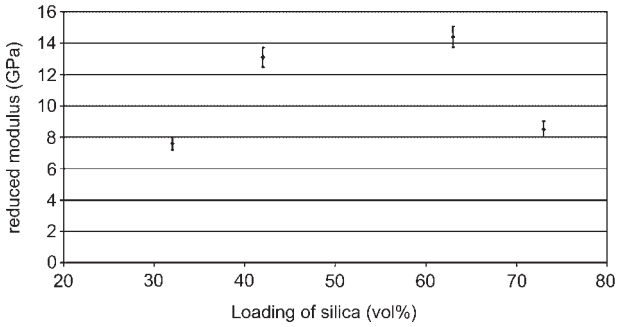

Figure 1. Reduced modulus of elasticity of a nanocomposite TMPTA film at different SiO_2 packing densities, exhibiting a maximum at about 60 vol % nanoparticle loading.

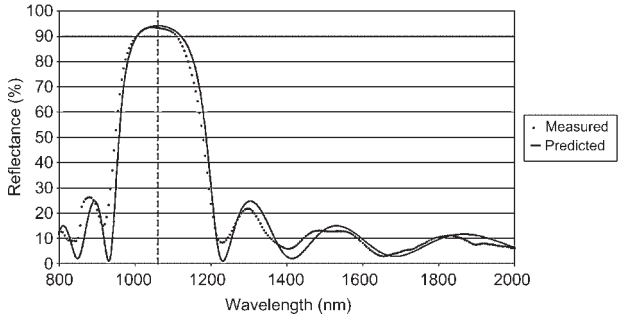

Figure 2. Measured and predicted reflectance spectrum of the 15 layer stack.

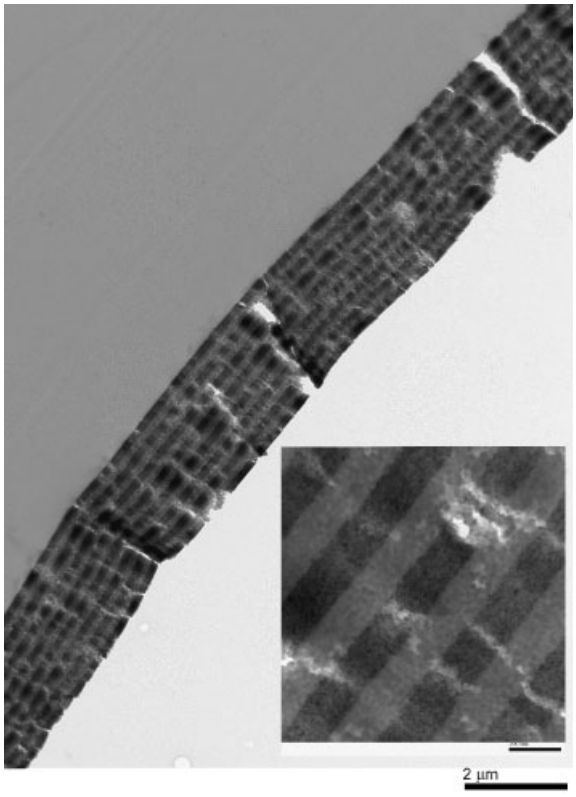

Figure 3. Cross-section TEM image of the nanocomposite infrared filter, where the dark section is the TiO_2 and the lighter section is SiO_2. Inset is a closer view (approximately 10 × magnification) showing the nanoparticles embedded in the polymer matrix.

A thin-film stack was designed to have a reflectance of greater than 90% at a wavelength of 1060 nm; the stack based on the two nanocomposite materials required fifteen layers. (A conventional TiO_2/SiO_2 CVD stack would require nine layers.) The corresponding ¼ wave thicknesses of these films are 180 nm and 140 nm for the low and high refractive index layers. The resulting reflectance from the surface is shown in Figure 2 and compares very well with the predicted response.

Thin cross-sections of the stack on a polycarbonate substrate were used to verify layer thickness and interlayer adhesion. The coated polycarbonate substrates were shaved with a microtome to produce 50–150 nm thin cross-sections, which were analyzed by transmission electron microscope TEM (JEOL 2010F TEM). Figure 3 shows that the total thickness is approximately 2.4 μm, which agrees with the stack design of eight layers at 140 nm and seven layers at 180 nm. The insert in Figure 3 shows individual nanoparticles.

The micrograph also shows that the coating performs well at points of high stress, as is evident from the nature of the tearing of the sample that occurs during the microtome process. In the torn areas, there is no evidence of failure along the interlayer surfaces, confirming good interfacial adhesion within the stack. In addition, there is one tear that terminates at the substrate, where it is likely that the propagation is along the substrate–nanocomposite interface.

Elemental mapping (electron energy-loss spectroscopy (EELS); JEOL 2010F TEM) was conducted on a two-layer nanocomposite of low- and high-index nanocomposites. Figure 4 shows that the separation between the high-and low-index layers is well defined and confirms the existence of the polymer in the nanocomposite layers.

The modulus of PVD and sol–gel coatings is well matched to glass, but significantly larger than a polymer substrate such as polycarbonate or PMMA,[3,15,16] whereas the polymer nanocomposite is mechanically well matched. The metal oxide nanoparticles embedded in the film increase the elastic modulus, providing a thin ''hard'' coat over the softer material, while maintaining the ratio of mechanical properties

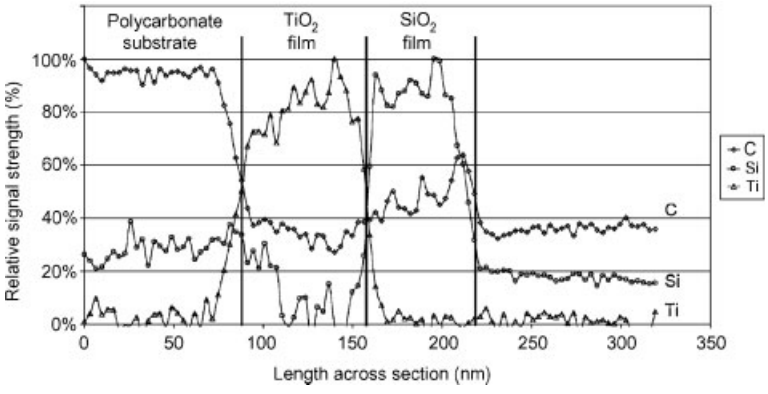

Figure 4. Elemental mapping of a two-layer stack conducted using three elements: titanium, silicon and carbon. Each element is mapped by the ratio of the signal strength (counts) to the maximum signal for that element expressed as a percent.

to those of the polymer substrate close to unity. This closely matched strain domain limits the stress-induced cracks that occur under large deformations.

We have shown that polymer–nanoparticle-composite thin films can be used effectively to produce infrared mirrors using a simple, scalable, and inexpensive process. Additionally these films have better strain capabilities making them suitable for plastic and flexible substrates and for systems that undergo thermal cycling. In addition, the spin process allows for higher layer stack designs to be successfully applied to curved substrates without affecting the performance. The nanocomposite coatings have been successfully demonstrated for the ultraviolet through to the near-infrared range using nanoparticles of metal oxides. This method could also be used with other nanoparticles which would have better properties in the infrared spectrum, such as metals and nitrides of metals.

Experimental Section

Ultrathin nanocomposite films were manufactured by spin-coating onto a plastic substrate using a dispersion containing nanoparticles, monomer, initiator, and solvent. Spin-coating controls the layer thickness by balancing the centrifugal forces on a spreading thin film with the viscous forces that increase as evaporation takes place, yielding very good repeatability.[17,18] The layer is then partially cured using a pulse Xenon UV source lamp, creating a polymer nanoparticle composite. Monomer conversion in the uppermost layer is controlled to be less than 100%, so that monomers in the following layer will crosslink across the interfacial zone, improving interlayer adhesion. Good interfacial adhesion between layers formed by such processing has been shown by nanoindentation studies.[19]

The spin-coater used was manufactured by Optical Dynamics and is capable of spinning a substrate at 1000 to 2000 rpm. The environment is a temperature-controlled HEPA air space set between 25 °C and 35 °C and includes a coating chamber that is equipped with an exhaust blower to enhance solvent evaporation and minimize defects. In addition the apparatus includes a high-pressure cleaning station and a 1600 W s pulse Xenon strobe in the curing station. The machine has a robotic arm that is designed to move 4–80 mm round substrates through a multi-step coating process that includes cleaning, coating, and curing. The low-index film is composed of an acrylate monomer nanoparticle silica dispersion received from Hansie-Chemie Industries (XP270) and combined with a silica colloid as supplied by Nissan Chemicals (IPA-ST). The colloid improves the bonding between the silica nanoparticles and the acrylate, increases the packing density of nanoparticles, and improves the mechanical performance of the final film. The monomer is a trimethylol propane triacrylate (TMPTA). The photoinitiator is a benzoyl cyclohexanol supplied by Ciba as Irgacure 184. *n*-propanol (Sigma–Aldrich) was used for its compatibility with the colloid and to minimize defects caused during the spin process.

The high-index film was a nanocomposite composed of anatase titania, TMPTA (Sartomer 351), a photoinitiator (Ciba Irgacure 184) and solvent (*n*-propanol Sigma–Aldrich). The titania was made in our laboratory using a hydrothermal process.[20] The titania nanoparticles ($D \approx 20$ nm) were functionalized to improve their dispersion in the coating solution, and to improve their adhesion to the polymer matrix. In both cases the solids are added to the solvent dropwise under stirring.

Using the apparatus and solvent systems described above requires between 3% and 10% solid concentrations to create layers of the order of 100 and 200 nm, respectively. The fine tuning of the thicknesses was handled by adjusting the spin speeds between 1000 and 2000 rpm. The thickness of the thin films was established using a contact profilometer model XP2 by Ambios Corporation measuring the step height of the film scraped from a glass substrate.

The spectral response of the films was characterized using a Beckman Coulter Model 800 spectrophotometer in the range of 800–2000 nm. The refractive index of each of the two layers was determined to be 1.48 for the low-index layer and 1.88 for the high-index layer, which is lower than expected for high-index layers and could result from impurities or insufficient packing. The refractive index was established from the measured thickness and the reflectance spectrum, then by using TFCalc by Software Spectra, Inc. to compute a refractive index. In some cases several layers are required in order to get an accurate refractive index measurement.

Keywords:

infrared · nanocomposites · refractive index · thin films

[1] D. A. Glocker, S. I. Shah, *Handbook of Thin Film Process Technology*, IOP, Bristol, UK **1995**.
[2] J. L. Vossen, W. Kern, *Thin Film Processes*, Vol. *2*, Academic, New York **1991**.
[3] L. Martinu, D. Poitras, *J. Vac. Sci. Technol. A* **2000**, *18*, 2619.
[4] K. M. Chen, A. W. Sparks, *Appl. Phys. Lett.* **1999**, *75*, 3805.
[5] M. Mennig, *Thin Solid Films* **1999**, *351*, 225.
[6] I. M. Thomas, P. W. Oliveira, A. Frantzen, in *Laser-Induced Damage in Optical Materials*, SPIE, Bellingham, WA 1993, p. 1994.
[7] D. S. Hinczewski, M. Hinczewski, F. Z. Tepehan, *Sol. Energy Mater. Sol. Cells* **2005**, *87*, 181.
[8] S. Grego, J. Lewis, E. Vick, *Thin Solid Films* **2007**, *515*, 4745.
[9] Y.-W. Rhee, H.-W. Kim, Y. Den, *J. Am. Ceram. Soc.* **2001**, *84*, 1066.
[10] T. Druffel, K. Geng, E. Grulke, *Nanotechnology* **2006**, *17*, 3584.
[11] T. Druffel, X. Sun, K. Krogman, Lens Forming Systems and Methods, U.S.P. Application, 11/203,422 2006.
[12] K. Krogman, T. Druffel, M. Sunkara, *Nanotechnology* **2005**, *16*, S338.
[13] H. A. Macleod, *Thin Film Optical Filters*, IOP, London **2001**, p. 641.
[14] J. Malzbender, J. M. J. den Toonder, A. R. Balkenende, *Mater. Sci. Eng. R* **2002**, *36*, 47.
[15] R. Saha, W. D. Nix, *Acta Mater.* **2002**, *50*, 23.
[16] J. S. S. Wong, H. J. Sue, K. Y. Zeng, *Acta Mater.* **2004**, *5*, 431.
[17] D. E. Bornside, C. W. Macosko, L. E. Scriven, *J. Appl. Phys.* **1989**, *66*, 5185.
[18] D. Meyerhofer, *J. Appl. Phys.* **1978**, *49*, 3993.
[19] T. Druffel, K. Geng, E. A. Grulke, *Nanotechnology* **2006**, *17*, 3584.
[20] N. Mandzy, E. A. Grulke, T. Druffel, Methods of Making and Using Metal Oxide Nanoparticles, U.S.P. Application 60/738, 642 Office.

Received: August 10, 2007
Published online: March 25, 2008

